

Substance-related investigation of the evaporation characteristics of free falling alkane-ethanol droplets using Raman spectroscopy

Thomas Hillenbrand*, Dieter Brüggemann

University of Bayreuth, Chair of Engineering Thermodynamics and Transport Processes (LTTT), Bayreuth Engine Research Center (BERC), 95440 Bayreuth, Germany

*Corresponding author: LTTT@uni-bayreuth.de

Abstract

A detailed understanding of the evaporation process is a key issue in the design of internal combustion engines. The emerging of renewable fuels has led to recent challenges in the prediction of this process in particular for blended fuel sprays. In this context, the blending of ethanol into gasoline in various substance ratios is an already widely spread approach. Even though these mixtures are already in use, the evaporation process of these fuel blends is still insufficiently characterized. The particular occurrence of component-by-component evaporation compromises the efficient and the low-emission operation of internal combustion engines due to inhomogeneous mixture formation. In order to meet these challenges, a precise understanding of the mechanisms causing the component-by-component evaporation is inevitable. Initially, a precise and extensive experimental investigation is essential. Referring to this, to identify the fundamental mechanisms raising these challenges, the evaporation of droplets under controlled conditions needs to be considered first. Available sources for experimental validation focus on lying or levitated droplets. Therefore, the emphasis of this work is the experimental evaluation of the component-by-component evaporation of free falling droplets consisting of various binary mixtures of n-hexane, iso-octane or n-decane blended with ethanol. A high-resolution Raman setup combined with a fast triggering system is established. The gaseous phase directly behind free falling droplets is resolved quantitatively and substance-related. To ensure engine-like conditions, the droplet diameter is kept below 60 μm . Single droplets as well as droplet chains and an intermediate droplet character are investigated. A systematic variation of the droplet temperature, the falling distance, the droplet generating frequency and the relative ratios of the applied substances are accomplished. The evaluation reveals that the component-by-component transfer into the gaseous phase is strongly depending on the adjusted parameters and the applied substances. Furthermore, the results indicate a depletion of the more volatile substance at the droplet surface with increasing droplet temperature at selected component ratios.

Keywords

Droplet evaporation, free falling droplet, ethanol, Raman spectroscopy, mixture formation

Introduction

The aspiration to reduce the reliance on fossil fuels contributes to an increasing interest in alternative fuels. In addition, increasingly stricter environmental regulations on pollutant emissions in the mobile sector urge for a continuous improvement in the efficient and the low-emission operation of internal combustion engines.

In this context, ethanol has become one of the most promising renewable fuels. Ethanol can be produced from sugary, starchy and cellulosic biomass [1, 2]. Therefore, a diversity of production processes is present to cover a growing demand. Nevertheless, great progress has been achieved in the production via algae to minimize the impact on the environment and the competition with food production [3–8].

However, the blending of ethanol to gasoline is an already widely spread approach today. Gasoline blended with 10 vol.-% ethanol is applied in Germany, France, Finland and other countries. Higher ethanol ratios are also common, for instance, in the USA and Brazil. This wide dissemination of the application of blended gasoline is not only attributable to the CO₂ neutral production process of ethanol but also to the advantages deriving during the combustion process. Due to the higher octane number of ethanol in comparison to pure gasoline, these blends offer the opportunity to decrease the CO₂ and the NO_x emissions while simultaneously improving the engine efficiency and the combustion stability as a result of the presence of oxygen within the fuel molecule [9–12]. However, the evaporation process of fuel blends is still insufficiently characterized [13–16]. The blending with ethanol has a decisive influence on the evaporation process and on the mixture formation inside a combustion engine. Therefore, known advantages are accompanied by significant challenges. Without a detailed understanding of the evaporation behaviour, the blending with gasoline into an unadjusted combustion engine can lead to an inhomogeneous component distribution and thus to a rise of the emitted NO_x and CO emissions, thermal stress, increased fuel consumption and the generation of acetaldehydes [9].

As the evaporation behaviour and the mixture formation are of significant relevance for an aspired efficient and low emission operation of a combustion engine, extensive fundamental research has been performed in the last decades. Numerical investigations as well as experimental research have been performed for binary and multicomponent mixtures for droplets and sprays [17–26]. However, this existing work needs to be extended for characterizing the evaporation of fuel blends containing ethanol in various ratios [30–33] as different ethanol ratios blended into gasoline lead to best results depending on application like power generators, automobiles, construction machines or trucks [27].

However, the blending of ethanol to gasoline in higher ratios causes the occurrence of component-by-component evaporation. This means that the substance composition inside a droplet is locally diverging from the substance composition that is transferred into the gaseous phase. Therefore, under conditions causing a pronounced component-by-component evaporation, an inhomogeneous substance distribution arises. Ghassemi et al. [28] reported this issue even for mixtures of alkanes of different boiling points. The impact of this effect is even more pronounced for non-ideal mixtures of polar and nonpolar substances with onward diverging boiling points [29] like blends of ethanol and alkanes.

However, the available literature for experimental validation focuses on lying or levitated droplets, missing detailed information of air enrichment in the droplet drag phase at small droplet spacing and the influence of turbulences close to the droplet. Yet, the major advantages and disadvantages of fuel blends occur in particular at cold start conditions. Due to low temperatures inside the combustion chamber, the mixture formation is impaired. Therefore, the combustion process at cold start is performed under rich conditions to avoid misfire. Thus, the amount of emissions produced during the cold start phase rises dramatically. Chen et al. [30] showed that the addition of 20–40 vol.-% ethanol to gasoline allows a less rich condition at cold start conditions. The leaner conditions lead to less unburned HC and less CO emissions. In contrast, the component-by-component evaporation is more pronounced for low temperatures increasing its impact and the demand of investigation.

The mechanism is strongly influenced by adjacent droplets, the substance ratio in the ambient air as well as the temperature, turbulences and the falling distance [31]. For this reason, this phenomenon is difficult to predict and experimental data are needed for comparison. In addition, numerical models typically rely on simplifications to predict the evaporation process of pure gasoline. It is unclear which assumptions are valid for multicomponent mixtures like a blending with ethanol.

Therefore, in this study the occurrence and the impact of the component-by-component evaporation under low temperatures has been investigated at free falling droplets for the first time. Binary mixtures of hexane, octane and decane are blended with ethanol in relevant ratios up to 85 vol.-% ethanol. The major influencing parameters are investigated under controlled conditions. Non-intrusive optical measurement techniques are applied to achieve a quantitative evaluation of the substance ratio in the gaseous phase directly behind the falling droplet.

Preparatory work

In order to achieve an application-oriented investigation, preferably small droplets are desirable. However, the handling of very small droplets with a diameter below 60 μm represents challenges to the measurement methods and to the droplet generation itself. In addition, the investigations are performed under cold start conditions. Consequently, low ambient temperatures and a low evaporation rate are implied. The concluding low signal intensity and the low signal to noise ratio necessitate an accumulation of 6000 individual laser pulses for one measuring point in order to produce reliable results.

Therefore, the measurements are carried out on stable droplet chains with different droplet spacing. This way, the measurement conditions at the free falling droplets as well as the generated droplets present highest reproducibility. This is particularly important, as smallest air movements affect the trajectory of the droplets, which impedes the investigation and complicates the creation of controlled and consistent conditions. Furthermore, it is indispensable that monodisperse droplets are produced and that satellite droplets are avoided. A failure to comply with these conditions would lead to a significant impairment of the results. The generation of satellite droplets could also lead to an impingement between the laser and a satellite droplet. This could lead to a plasma breakdown and damage the camera, or even ignite the droplet chain. Appropriate preparatory work is therefore performed to ensure that these conditions are met.

For this purpose, the droplet generation is verified first. A piezoelectric DOD (droplet on demand) droplet generator is applied. In this case, precisely defined droplets are generated by applying a defined voltage (level and length of a pulse) to the piezoelectric element. Hereby, the different droplet characters can be generated through different droplet generation frequencies. At high generation frequencies, the spacing between the free falling droplets is very small. Therefore, a droplet chain character is present. With increasing spacing and decreasing generation frequency, the single droplet character rises. In this study, single droplets (20 Hz), droplet chains (700 Hz) and an intermediate character (100 Hz) are investigated. However, the surface tension, the density and the mixing ratio of the applied fluids have a large influence on the droplet generation. The most important parameters of the applied substances are listed in Table 1.

Table 1. Physical and chemical properties of the applied substances [32]

Specification	Ethanol	n-Hexane	Isooctane	n-Decane
Molecular formula	C ₂ H ₆ O	C ₆ H ₁₄	C ₈ H ₁₈	C ₁₀ H ₂₂
H/C – ratio	3.00	2.33	2.25	2.20
Molar mass (g/mol)	46.1	86.2	114.2	142.3
Boiling point (K)	351	342	372	447
Density at 293 K (g/cm ³)	0.79	0.66	0.69	0.73
Surface tension at 293 K (g/s ²)	21.9	18.3	16.7	21.8
Vapour pressure at 293 K (kg/m·s ²)	58·10 ²	162·10 ²	51·10 ²	2·10 ²

As some of these parameters depend on the temperature, suitable generation settings have to be located for each individual measuring point. For this reason, a shadow microscope is set up to verify the properties of the droplets. The droplet speed, the diameter, the monodispersity and the absence of satellite droplets are verified. Additionally, it has been determined that no noticeable change in the droplet diameter occurs during the examined falling distance of 5.0 mm. In addition, the exact droplet diameter and the droplet speed can be recorded for each measuring condition. This way the droplet spacing is determined.

Reference Measurements

In order to assign the Raman signals to the respective component ratio and to achieve a quantitative and a substance-related evaluation, reference measurements of the applied pure substances and various binary mixtures in small intermediate steps are mandatory. This way a quantitative evaluation of the gaseous phase behind the free falling droplets is achieved. These measurements are performed at optically accessible and sealed measuring cylinders filled with a defined and known substance composition in the gaseous phase. The measurements are performed with a frequency doubled, Q-switched Nd:YAG laser (532 nm) combined with a spectrograph (Triax 320, HORIBA Jobin Yvon GmbH) including an optical grating with 600 lines per millimetre.

The CH₂ and CH₃ stretching vibrations of the contained hydrocarbon-bonds of the applied substances are detected as they show the highest signal intensity. As hydrocarbon-bonds are contained in ethanol as well as in all applied alkanes, the Raman signals overlap additively in the Raman shift of 2800 to 3000 cm⁻¹. However, the pure substance spectra of the alkanes and the pure substance spectra of ethanol differ sufficiently to distinguish. Additionally, a continuous transition between both pure substance spectra is evident.

To optimize the evaluation, an appropriate processing of the raw spectra is performed. An internal dark image correction is implemented as a first step. After that, a flat-field correction followed by an averaging on the intensity axis on the imager is carried out. Furthermore, a background adaption is performed due to non-suppressible scattered radiation and a 2nd polynomial Savitzky-Golay smoothing is applied. Upon completing the corrective actions, the cumulative Raman bands are fitted with a multi-pulse fit using Voigt functions. The natural line shape and possible superimpositions of the device function are taken into account. The resulting area of the multi-pulse fit equates to the intensity of the cumulative Raman line. This way, a correlation between the areas of the multi-pulse fit and the content of ethanol within the mixture can be determined. The processed reference images are shown in Figure 1.

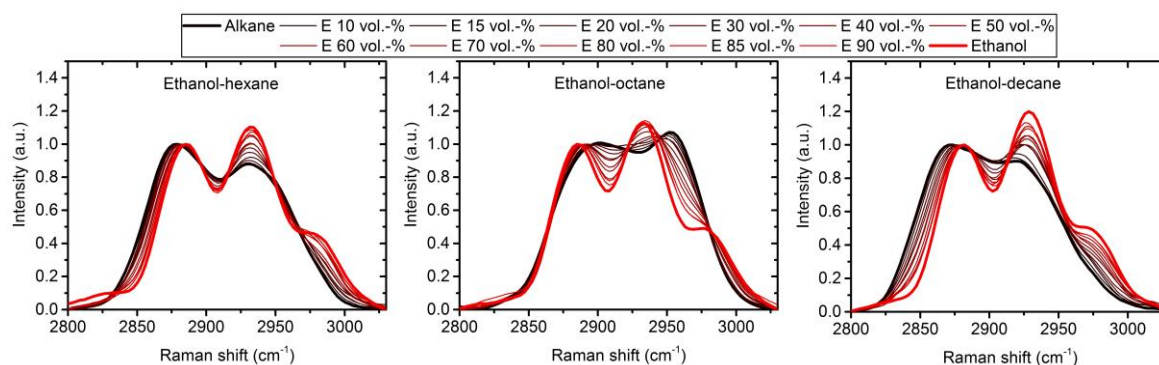


Figure 1. Processed Raman scattered light of reference measurements of various volumetrically mixed binary blends of ethanol and the respective alkane and pure substances in the gaseous phase.

Experimental setup

The actual measurements at the free falling droplets are performed at the experimental arrangement, which is shown in Figure 2. The influences of the droplet initial temperature, the spacing between droplets, the falling distance and the mixing ratio of the components inside the droplet are investigated. The frequency doubled, Q-

switched Nd:YAG laser (532 nm) applied to the arranged high-resolution Raman spectroscopy setup is extended with a fast triggering system to synchronise the laser and the falling droplets in order to avoid a direct impingement of the laser into the droplet. The droplets are detected while falling through an additional triggering laser combined with a photodiode (Figure 3). The Nd:YAG laser is triggered with a short delay after the intensity of the trigger laser has dropped and the camera is synchronized to the release of the Nd:YAG laser. The delay between the trigger and the release of the laser pulses and the camera is adjustable. This way, the distance between the measuring spot and the falling droplet is consistent and comparable.

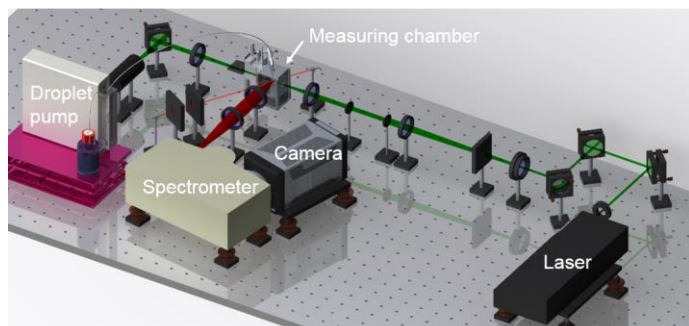


Figure 2. Experimental arrangement of the Raman setup combined with a fast triggering system

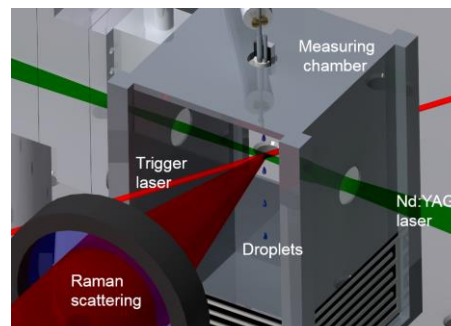


Figure 3. Enlarged illustration of the measurement chamber and the falling droplets

The measurements are performed at an optically accessible measuring chamber to reduce the influence of air movements and to guarantee a constant ambient temperature. An enrichment inside the measuring chamber is eliminated due to the very low evaporation rate compared to the size of the chamber. In addition, this is checked before and after each measurement. To ensure engine like conditions, a droplet diameter below 60 μm is applied. Therefore, the initial droplet diameter of the generated droplets is kept equal and the droplet velocity diverges slightly during the fall, as the monodisperse droplet generation is limited to a small section of input parameters for the droplet generator. The ambient temperature is kept at 293 K. The initial droplet temperature is varied, as a rise of the ambient temperature inside the measuring chamber results in an uncontrollable air circulation. The applied experimental conditions are shown in Table 2.

Table 2. Experimental properties and applied experimental conditions

Specification	Parameter
Ethanol content (vol.-%)	10 / 50 / 85
Initial droplet temperature for hexane and octane 90 vol.-% (K)	293 / 323
Initial droplet temperature for decane and octane 15 and 50 vol.-% (K)	323 / 353
Ambient temperature (K)	293
Distance, measurement spot to droplet generation (mm)	1.5 / 5.0
Generating frequency (Hz)	20 / 100 / 700
Droplet diameter (μm)	50 – 59

Theory

The inhomogeneous substance distribution inside a combustion chamber is one of the most important challenges for the application of higher ethanol ratios blended in gasoline. Hereby, regions that are highly concentrated with ethanol and regions that are highly concentrated with gasoline are formed. This is schematically shown in Figure 4. Most notably for small droplets under cold start conditions, the component-by-component evaporation has a decisive influence on the substance distribution. During this mechanism, the composition of the evaporating gaseous phase and the initial composition inside the droplet differentiate. Consequently, the contained substances inside a droplet are unevenly transferred into the gaseous phase considering a complete evaporation of the droplet. This mechanism is assumed to be explained as follows.

As one substance is preferably transferred into the gaseous phase, the composition of the gaseous phase and the initial composition inside the droplet are diverging. Therefore, the ratio of the more volatile substance decreases inside the droplet. For non-turbulent conditions under low temperatures, the evaporation typically takes place at the droplet surface. Consequently, the less volatile substance is concentrating at the droplet surface as the more volatile component is transferred into the gaseous phase. Therefore, the composition in the droplet centre remains constant in the first place. This behaviour is maintained as long as the composition at the droplet surface is not changed significantly. At a certain point, the less volatile substance becomes increasingly concentrated at the droplet surface. Consequently, an inner diffusion flow is developed due to the concentration gradient inside the droplet. This balance between inner mass transfer (diffusion of the more volatile substance from the droplet centre to the droplet surface)

and the evaporation rate (transfer of the more volatile component into the gaseous phase at the droplet surface) regulates the substance composition at the droplet surface. This balance can be maintained the longer, the more of the more volatile substance is present. It is directly influenced by experimental conditions and the initial droplet composition. Therefore, for blends with little amount of the more volatile substance, it is conceivable that an impoverishment of the more volatile component at the droplet surface takes place even for very short falling distances although only small quantities of the fluid are transferred into the gaseous phase and the droplet diameter is nearly unchanged. This might happen under certain conditions, when the evaporation rate exceeds the inner diffusion rate.

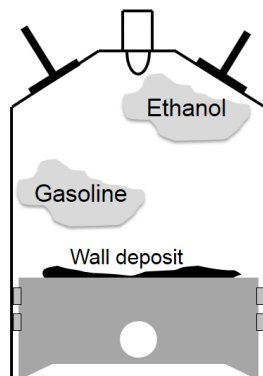


Figure 4. Schematic illustration of inhomogeneous substance distribution inside a combustion chamber of gasoline blended with ethanol.

This modification of the substance ratio at the droplet surface is accordingly affecting the evaporation. While a huge amount of the more volatile substance is present at the droplet surface, it will dominate the evaporation and the gaseous phase. By the time, the ratio of the more volatile substance is decreasing at the droplet surface the dominance of the more volatile substance in the gaseous phase is diminishing. Under that condition, the less volatile substance dominates the gaseous phase. This way, regions highly concentrated with ethanol and regions highly concentrated with the respective alkane may be formed.

Besides, the high evaporation enthalpy of ethanol increases the probability of spray-wall interactions and wall deposits under low temperatures. In this context, the composition of the wall deposit is strongly diverging from the initial fuel composition and is therefore amplifying the separation due to the preceding component-by-component evaporation.

The occurrence of component-by-component evaporation is a typical characteristic for small droplets at low temperatures. However, this mechanism is strongly influenced by turbulences inside and around the droplet, the properties of the applied substances, the enrichment of the ambient air and the mixing ratio of the applied substances. Therefore, the details of evaporation on become difficult to predict for application orientated measurements as simplifications, which are often applied in numerical models, might not take all of these influences into account. Therefore, the experiments performed in this work focus on the component-by-component evaporation and the central question how this behaviour is influenced.

Results and discussion

As first step approaching this issue, interesting mixture compositions are identified. Therefore, all measured data are depicted in Figure 5. In this diagram, the respective ethanol to alkane ratio measured directly behind the free falling droplet is shown on the y-axis. The initial composition inside the droplet is shown on the x-axis. This initial composition is additionally represented graphically as a dashed line for improved clarity. Measured data above this dashed line represent a higher ethanol ratio in the gaseous phase in comparison to the initial droplet composition. Therefore, measured data below that dashed line represent a domination of the respective alkane in the gaseous phase.

It is not distinguished between different initial temperatures, generation frequencies and falling distances of the droplets. All measured data are illustrated composed for each initial mixture ratio. As the experimental conditions are altered in the same extent for each mixture ratio, the range of the measured data equates the suggestibility of each mixture composition. Consequently, initial mixture compositions that show a large range of ethanol ratio in the gaseous phase are most likely to be influenced and therefore are most suitable to investigate the influences and the ongoing mechanisms, as the influence is most visible.

In Figure 5, the majority of the measured data for each mixture of ethanol and hexane are shifted into an area with higher hexane ratio in comparison to the initial droplet composition. Therefore, a higher volatility of hexane is specified. This is attributed to the higher vapour pressure of hexane in comparison to ethanol. Single exceptions can be noticed for ethanol to hexane 10/90 vol.-% and 85/15 vol.-%. These seem to be affected by the experimental conditions (temperature, droplet character, falling distance).

For blends of ethanol and octane, a contradictory behaviour is shown. The mixture of 10 vol.-% ethanol depicts a higher volatility of ethanol while octane is dominating the evaporation for mixtures of 50 vol.-% and 85 vol.-% ethanol. The data measured in the gaseous phase do not diverge significantly from the initial droplet composition. This can be explained due to the almost equal vapour pressure of octane and ethanol.

For blends of ethanol and decane, a domination of ethanol in the gaseous phase can be seen. Again, this can be explained referring to the high vapour pressure of ethanol in comparison to the one of decane. The blend of ethanol 85 vol.-% shows single exceptions.

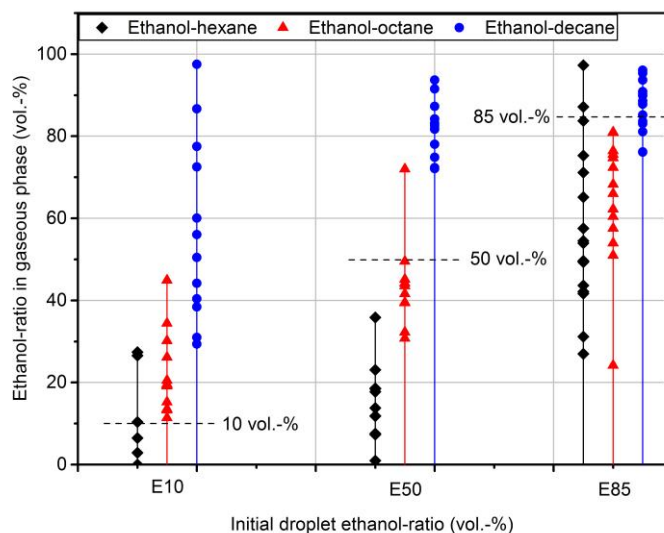


Figure 5. Ethanol ratio in the gaseous phase measured directly behind free falling droplets of mixture ratios of 10 vol.-%, 50 vol.-% and 85 vol.-% ethanol in relation to the respective alkane hexane, octane or decane. The measured data are illustrated for the investigated falling distances 1.5 mm and 5.0 mm, the respective initial droplet temperatures 293 K and 323 K or 323 K and 353 K and the droplet generation frequencies 20 Hz, 100 Hz and 700 Hz.

Concerning the range of the measured data, it is evident that most blends show a range of the ethanol to the respective alkane ratio of less than 40 vol.-%. These blends are ethanol to hexane 10/90 vol.-% and 50/50 vol.-%, all ethanol to octane blends and ethanol to decane 50/50 vol.-% and 85/15 vol.-%. In contrast, the blends ethanol to hexane 85/15 vol.-% and ethanol to decane 10/90 vol.-% show a range of about 70 vol.-% and obvious divergences of the measured values.

This wide range in addition to the diverging composition between the gaseous phase and the initial composition inside the droplet and the preferential transfer of one substance into the gaseous phase are indications for an influence of the component-by-component evaporation and the surface near depletion in reference to the nearly unchanged droplet diameter.

The blend ethanol to hexane 85/15 vol.-% is therefore discussed subsequently to investigate the occurrence and the influence of component-by-component evaporation and the surface near depletion. To identify the influence of the varied experimental conditions, the measured data are shown in Figure 6 and Figure 7. The ethanol ratio in the gaseous phase measured directly behind the free falling droplets is shown on the y-axis and the droplet generation frequency and the droplet falling distance (Figure 6) respectively the initial droplet temperature (Figure 7) are shown on the x-axis. The influence of the initial droplet temperature is shown in Figure 6. Therefore, the initial droplet temperatures 293 K and 323 K are compared under otherwise identical conditions. In direct comparison of both temperature levels, an increased ethanol ratio in the gaseous phase is obvious for the measured data received at 323 K. This increase is obvious for all falling distances and generating frequencies. An exception is shown at 100 Hz, 323 K and 5.0 mm. The examined droplets are significantly slower. Thus, a deviant evaporation characteristic is observed. To generate monodisperse droplet chains, the generation parameters in the droplet generator are adjusted for each temperature due to changing surface tensions. To assure an equal droplet diameter, the droplet velocity is modified at this operating point.

The rising ethanol ratio with increasing temperature by 30 K represents a decrease of the hexane ratio by implication. This can be explained as follows. As the composition of the evaporating gaseous phase is distinguishing from the composition of the droplet, the hexane ratio at the droplet surface inside the droplet edge is decreasing. The balance between inner mass transfer and component-by-component evaporation regulates the extent of the decrease. The rising temperature results in an increase of the evaporating mass. Therefore, the evaporation predominates the balance at higher temperatures. The impoverishment at the droplet surface is extended, resulting in a decreasing amount of hexane in the gaseous phase.

In addition, it can be seen that the majority of the measured data are shifted into an area of less ethanol in the

gaseous phase in comparison to the initial ethanol ratio of 85 vol.-% in the droplet. As depicted before, the gaseous phase is dominated by hexane. However, the maxima of the measured ethanol ratio stand out for a droplet generation frequency of 20 Hz and a falling distance of 5.0 mm. The respective maxima are located at 87 vol.-% ethanol for 293 K and at 97 vol.-% ethanol for 323 K. The other data are settled between 25 vol.-% and 65 vol.-% ethanol to hexane ratio.

These high ethanol ratios occur at single droplets with wide droplet spacing and for the longest investigated falling distances. Regarding the surface near depletion, this behaviour can be explained. The impoverishment at the droplet surface is extended for longer falling distances. For single droplets, (20 Hz generating frequency) this behaviour is intensified due to the missing enrichment of the ambient air. Therefore, it is probable that the surface near depletion has become so extended that almost all hexane at the droplet surface is transferred into the gaseous phase. Ethanol is concentrating at the droplet surface and therefore dominating the gaseous phase under the studied conditions.

It is mentionable that this behaviour occurs even within a very short falling distance of 5.0 mm. Within the varied investigated parameters, an ethanol ratio in the gaseous phase between 27 vol.-% and 97 vol.-% is evident. Concerning engine applications and longer falling distances, this range is presumably even wider. However, the investigation performed in this study shows that the component-by-component evaporation is present under cold start conditions already at very short falling distances. While almost pure ethanol is transferred into the gaseous phase for single droplets at certain falling distances, the evaporation is clearly dominated by hexane under slightly changed conditions.

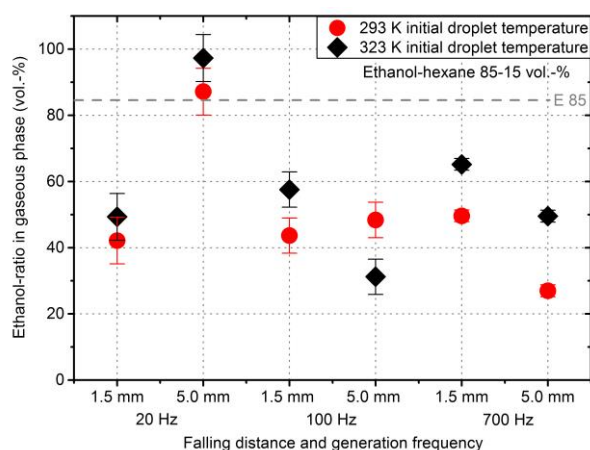


Figure 6. Relative ethanol ratio in the gaseous phase of a droplet with an initial substance ratio of ethanol to hexane 85/15 vol.-%. The initial droplet temperatures of 293 K and 323 K are compared under otherwise identical conditions.

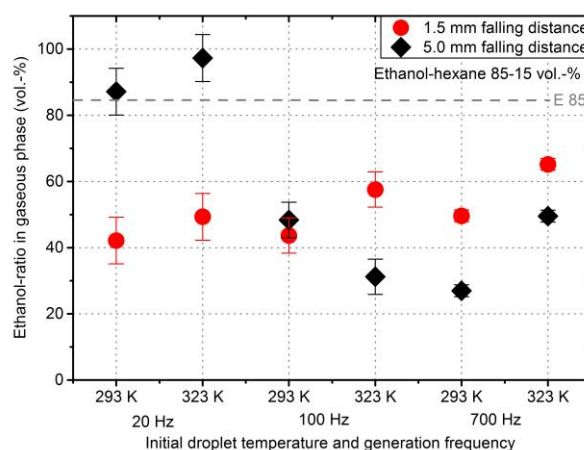


Figure 7. Relative ethanol ratio in the gaseous phase of a droplet with an initial substance ratio of ethanol to hexane 85/15 vol.-%. The falling distances of 1.5 mm and 5.0 mm are compared under otherwise identical conditions.

The influence of the droplet generation frequency is highlighted in Figure 7. Here, the same measured data are rearranged to compare the droplet falling distances. For single droplets (20 Hz droplet generating frequency), a significant increase of the ethanol ratio of about 40 vol.-% is evident while comparing both falling distances. The ethanol ratio at a generating frequency of 100 Hz is nearly constant for 293 K and decreasing for 323 K due to the affected data at 100 Hz, 323 K and 5.0 mm falling distance. The minor droplet velocity reveals a too low ethanol ratio in the gaseous phase. For droplet chains (700 Hz droplet generating frequency), a decreasing ethanol ratio of about 20 vol.-% is observed.

For droplet chains, the small droplet spacing leads to an enrichment of the ambient air until the succeeding droplet reaches the measuring point. The enrichment of the ambient air is depending of the substances transferred into the gaseous phase. Therefore, the ambient air is dominated by hexane. The presence of substances in the ambient air is affecting the evaporation and consequently the overall evaporation rate is reduced. Therefore, the surface near depletion is less extended or even not present. As a result, hexane is clearly dominating the gaseous phase.

This behaviour is enforced for longer falling distances as the droplets are slowed down and therefore the droplet chain character is increasing. Thus, the ethanol ratio is rising for droplet chains comparing the falling distances. With increasing single droplet character, the enrichment of the ambient air for the succeeding droplet is diminishing. Consequently, the hexane ratio in the gaseous phase is rising associated with a rising surface near depletion. For a generation frequency of 100 Hz, the transitional behaviour is evident at 293 K.

Concerning a spray ignition, typically various droplet characters are present. While the ambient air in the centre of the spray is enriched, the spray edge is equated with single droplets. Therefore, an inhomogeneous substance distribution is highly probable in blends with ethanol. With greater penetration depth, this effect may become increasingly critical if the spray conditions are not optimized for the applied fuel blend.

Conclusions

Extensive preparatory work has been performed to verify a feasibility of a quantitative investigation of the evaporation behaviour of free falling droplets in the first place. Binary blends containing ethanol and alkanes have been applied to determine the influences of the initial droplet temperature, the droplet falling distance, the droplet generation frequency and the ethanol ratio inside the droplet. The occurrence of component-by-component evaporation is observed under certain conditions. Furthermore, a strong dependence of the component-by-component evaporation on the external conditions is evident. The current results reveal that arbitrarily small differences of the initial conditions have a major impact on the substance distribution and the surface near depletion is indicated under certain conditions. The most important observations from the present study are summarized as follows:

- The evaporation process of binary mixtures of ethanol and n-hexane, iso-octane or n-decane can be investigated quantitatively and substance-related by observing the Raman bands of the contained hydrocarbons even under cold start conditions.
- The component-by-component evaporation is pronounced for blends of ethanol-hexane 85/15 vol.-% and ethanol-decane 10/90 vol.-% while it is not significant for other blends under the investigated conditions.
- For ethanol-hexane 85/15 vol.-% the increase in temperature by 30 K results in an increase of the ethanol ratio in the gaseous phase between 8–22 vol.-% under otherwise identical conditions. The mechanism of the surface near depletion of hexane is indicated.
- For ethanol-hexane 85/15 vol.-% a wider droplet spacing leads to a critical reduction of the hexane ratio in the gaseous phase while a shorter spacing increases the hexane ratio in the gaseous phase comparing the falling distances 1.5 mm and 5.0 mm. The influence of the enrichment of the ambient air is therefore determined.
- The relative ethanol ratio is influenced up to 75 vol.-% by the investigated experimental conditions. While almost pure ethanol is transferred into the gaseous phase for single droplets after a long falling distance, the gaseous phase is highly dominated by hexane for droplet chains at low temperatures. Therefore, pronounced component-by-component evaporation is evident.

References

- [1] Koç, M., Sekmen, Y., Topgül, T., Yücesu, H. S., 2009, *Renewable Energy* 34 (10): 2101–2106.
- [2] Böttcher, J., Hampl, N., Kügemann, M., Lüdeke-Freund, F., 2017, “Biokraftstoffe und Biokraftstoffprojekte.”
- [3] Soleymani, M., Rosentrater, K. A., 2017, *Bioengineering (Basel, Switzerland)* 4.
- [4] Kim, N., Jung, H., Chang, H., Lee, P., 2011, *Bioresource Technology* 102: 7466–7469.
- [5] Lee, S., Lee, J., 2012, *Journal of Industrial and Engineering Chemistry* 18: 16–18.
- [6] Ellis, J., Hengge, N., Sims, R., Miller, C., 2012, *Bioresource Technology* 111: 491–495.
- [7] Jones, C. S., Mayfield, S. P., 2012, *Current opinion in biotechnology* 23 (3): 346–351.
- [8] Hirano, A., Ueda, R., Hirayama, S., Ogushi, Y., 1997, *Energy* 22: 137–142.
- [9] Türköz, N., Erkuş, B., Karamangil, M. I., Sürmen, A., Arslanoğlu, N., 2014, *Fuel* 115: 826–832.
- [10] Brassat, A., Thewes, M., Müther, M., Pischinger, S., 2011, *Motortechnische Zeitschrift* 12: 988–995.
- [11] Masum, B. M., Masjuki, H. H., Kalam, M. A., Rizwanul, Fattah, I. M., Palas, S. M., Abedin, M. J., 2013, *Renewable and Sustainable Energy Reviews* 24: 209–222.
- [12] Turner, D., Xu, H., Cracknell, R. F., Natarajan, V., Chen, X., 2011, *Fuel* 90 (5): 1999–2006.
- [13] Tanvir, S., Biswas, S., Qiao, L., 2017, *International Journal of Heat and Mass Transfer* 114: 541–549.
- [14] Storch, M., Hinrichsen, F., Wensing, M., Will, S., Zigan, L., 2015, *Applied Energy* 156: 783–792.
- [15] Elfasakhany, A., 2015, *Engineering Science and Technology, an International Journal* 18 (4): 713–719.
- [16] Suarez-Bertoa, R., Zardini, A. A., Keuken, H., Astorga, C., 2015, *Fuel* 143: 173–182.
- [17] Sazhin, S. S., Kristyadi, T., Abdelghaffar, W. A., Heikal, M. R., 2006, *Fuel* 85: 1613–1630.
- [18] Al Qubeissi, M., Sazhin, S. S., Elwardany, A. E., 2017, *Fuel* 187: 349–355.
- [19] Sazhin, S. S., 2017, *Fuel* 196: 69–101.
- [20] Borghesi, G., Mastorakos, E., Devaud, C. B., Bilger, R. W., 2011, “Modeling evaporation effects in conditional moment closure for spray autoignition.”
- [21] Sazhin S. S., Elwardany A. E., Krutitskii P. A., Depredurand V., Castanet G., Lemoine F., et al., 2011, *Int J Therm Sci* 50 : 114–180.
- [22] Ju, D., Zhang, T., Xiao, J., Qiao, X., Huang, Z., 2015, *Energy* 86: 257–266.
- [23] Strotos, G., Gravaises, M., Therodorakakos, A., Vergeles, G., 2011, *Fuel* 90: 1492–1507.
- [24] Tonini, S., 2015, *International Journal of Thermal Sciences* 89: 245–253.
- [25] Ebrahimian, V., Habchi, C., 2011, *International Journal of Heat and Mass Transfer* 54: 3552–3565.
- [26] Sazhin, S. S., Elwardany, A., Krutitskii, P. A., Castanet, G., Lemoine, F., Sazhina, E. M., Heikal, M. R., 2010, *International Journal of Heat and Mass Transfer* 53: 4495–4505.
- [27] Phuangwongtrakul, S., Wechsato, W., Sethaput, T., Suktang, K., Wongwiset, S., 2016, *Applied Thermal Engineering* 100: 869–879.
- [28] Arabkhalaj, A., Azimi, A., Ghhassemi, H., Markadeh, R. S., 2017, *Applied Thermal Engineering* 125: 584–595.
- [29] Gavhane, S., Pati, S., Som, S., 2016, *International Journal of Thermal Sciences* 105: 83–95.
- [30] Chen, R., Chiang, L., Chen, C., Lin, T., 2011, *Applied Thermal Engineering* 31: 1463–1467.
- [31] Pradhan, T. K., Panigrahi, P. K., 2016, *Colloids and Surfaces A: Physicochemical and Engineering Aspects* 500: 154–165.
- [32] Deutsche Gesetzliche Unfallversicherung e.V., 2018, *GESTIS-Stoffdatenbank, Gefahrstoffinformationssystem der Deutschen Gesetzlichen Unfallversicherung*. <http://www.dguv.de/ifa/gestis/gestis-stoffdatenbank/index.jsp> ([cit. 2018-02-31]).